

Associations between the Rho kinase-1 catalytic and PH domain regulatory unit



John W. Craft Jr., Hua Zhang, Marc N. Charendoff, Jeffery T. Mindrebo,
Robert J. Schwartz*, James M. Briggs**

Department of Biology and Biochemistry, University of Houston, Houston, TX 77204, USA

ARTICLE INFO

Article history:

Accepted 25 September 2013

Available online 4 October 2013

Keywords:

Rho-associated kinase
ROCK
Docking
PH domain

ABSTRACT

Rho-associated kinase, or ROCK, is an important mediator of ventricular remodeling in cardiac hypertrophy. It has a kinase catalytic domain, a coiled-coil domain and a Pleckstrin-Homology domain (PH domain) with a C1 domain insert. The C-terminal region including the PH domain and C1 domain insert is involved in an autoregulatory role for ROCK. We sought to evaluate whether a self association complex could form using computational docking approaches. We found that both the PH domain and the C1 domain could dock with the catalytic domain and we further found that they could dock in poses that are complementary to each other forming a three domain complex. We also confirmed a binding response using a surface plasmon resonance experimental approach. Information about the regulation of ROCK might lead to new strategies to develop lead inhibitor compounds to modulate cardiac remodeling.

© 2013 Elsevier Inc. All rights reserved.

1. Introduction

Heart failure is the leading cause of combined morbidity and mortality in the United States and other developed industrial nations, with an estimated two-year mortality of 30–50% for the patients with advanced disease [1,2]. Pathophysiological cardiac hypertrophy is accompanied by reactive fibrosis and remodeling and is driven by a cascade of signaling through protein–protein complex formation. Recently, highly proliferative CD34+/CD45+ fibroblasts derived from monocytic, blood-borne precursor cells were shown to play a critical role in the development of fibrosis in a mouse model of ischemic/reperfusion cardiomyopathy (I/RC) similar to human heart disease [2]. The differentiation of human monocytes into fibroblasts *in vitro* occurs after transendothelial migration (TEM) induced by monocyte chemoattractant protein 1 (MCP-1). Rho-associated-kinase (ROCK1) a member of the Rho kinase family [3] has been implicated in cardiac hypertrophy and ventricular remodeling by Schwartz and coworkers [2,4–7]. Our ROCK1 knockout (ROCK1^{-/-}) mice did not impair compensatory hypertrophic response induced by pressure overload, but exhibited reduced perivascular and interstitial fibrosis which occurs 3

weeks after the aortic banding [5]. Blocking ROCK1 gene activity significantly reduced the amount of mononuclear cells that differentiated into fibroblasts by >20-fold [2]. ROCK1 influences the early stages of mammalian embryonic morphogenesis as observed in increased transcripts in cardiac mesoderm, lateral plate mesoderm, and neural plate. A known inhibitor of ROCK1, Y27632, disrupts the migration and differentiation of cardiomyocyte cells [6,8]. The role of ROCK1 in cellular remodeling and migration in scar tissue formation and the protective effects of ROCK1 knockout mice motivated our team to look for mechanisms of natural ROCK1 inhibition and processes that might activate it.

We have focused on Rho-associated-kinase (ROCK), a downstream effector of Rho which has two isoforms, ROCK1 (p160ROCK, ROKb) and ROCK2 (ROKα) which exhibit 65% amino acid sequence identity and 95% homology [3,9]. ROCK1 and ROCK2 cellular expression profiles have been shown to be largely consistent with one another except that the highest expression levels of ROCK2 are found in brain and muscle tissues. ROCK1 is also the only one of the two isoforms that undergo cleavage by Caspase 3 during the activation of the apoptotic pathways. Expression studies monitoring the transcription level of ROCK1 and ROCK2 in both of the ROCK knockout studies have been published [10]. In each study, neither ROCK1 nor ROCK2 were upregulated to compensate for the lack of the other isoform, showing that their expression levels are independently regulated. ROCK is activated by RhoA-GTP at the Rho Binding Domain (RBD) by a proposed mechanism that displaces the Pleckstrin-Homology domain (PH domain), in an auto-regulatory inhibitory mechanism of the kinase domain. We sought to evaluate whether the PH domain of ROCK1 could form a complex with

* Corresponding author at: 4800 Calhoun, H4003 SERC, Houston, TX 77204-5001, USA. Tel.: +1 713 743 6595.

** Corresponding author at: 4800 Calhoun, 402D HSC, Houston, TX 77204-5001, USA. Tel.: +1 713 743 8366; fax: +1 713 743 8351.

E-mail addresses: rjschwarz@uh.edu (R.J. Schwartz), jbriggs@uh.edu (J.M. Briggs).

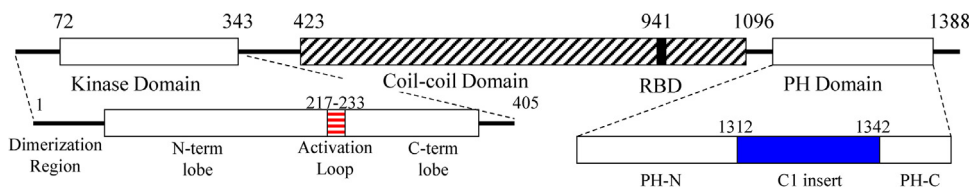


Fig. 1. Rho associated kinase (ROCK) domain schematic.

its catalytic domain using both computational and experimental approaches.

1.1. Topology and structure

Rho-dependent signaling is regulated by a family of Rho associated kinases or ROCKs. These serine-threonine kinases are composed of three domains including the N-terminal catalytic domain, followed by the coiled-coil region containing the RBD and then the C-terminal PH domain [3] (Fig. 1). ROCK's N-terminal helical subdomain mediates the interface for its native dimer organization [11,12] and was crystallized by Jacobs et al. (PDB: 2ETR) [11]. There are two isoforms of ROCK; ROCK1 and ROCK2. ROCK's genomic sequence is highly conserved among other species that also have ROCK and relative to other members of the kinase AGC family. Important members of that family that share the general organization of a N-terminal catalytic domain, a coiled-coil domain, and a C-terminal PH domain include DMPK, MRCK, and Citron kinase [13].

The N-terminal lobe of the catalytic domain consists of a five-stranded anti-parallel β -sheet and one α -helix, while the C-terminal lobe consists of 5 α -helices. The ATP binding pocket of the active site is located between the two lobes that are enclosed by the hinge region, the glycine-rich loop, and the activation loop. The activation loop of ROCK1 includes Asp117, Phe120, Arg197, Met221, Cys231, Asp232, and Thr233. Amino acids Lys105, Asn203, and Asp216 interact with ATP phosphates and Mg^{2+} ions. A salt bridge between Glu124 and Lys105 is conserved in catalytically active kinases.

The C-terminal domain of ROCK1 is categorized as a split PH domain with a C1 domain insert (Fig. 2). The binding of lipids to the PH domain is involved in ROCK's activation and localization in the cell, although these mechanisms for the split PH domain of ROCK1 are currently under investigation and are not well characterized. The C1 domain is inserted in the middle of the canonical PH domain, but neither domain interrupts the capacity for the other to properly fold [14]. Both domains display the same NMR chemical shift fingerprint, when purified independent or as a wild type full domain, demonstrating that each domain folds independently [14]. The split PH domain is composed of residues 1142–1342. The PH-N (N-terminal region) domain spans residues 1142–1227 and the PH-C (C terminal region) is defined from 1312 to 1342. The C1 domain insert is found between residues 1228 and 1311. The PH domain is split into two halves by the C1 domain, between β -strand 6 and β -strand 7. Other lipid binding PH domains tend to have a phosphoinositide binding region, which is absent in ROCK1. The Wen group [14] evaluated a region of the PH domain known to bind lipids in other proteins with similar PH domains, such as PKC. This region is found in the β 1/ β 2 loop and is comprised of positive residues in a general format of "KXn(K/R)XR" [14]. A lysine is found at the next to last position of β -strand 1 and the "(K/R)XR" region corresponds to positions 2 through 4 on β -strand 2 [14]. While ROCK1's PH domain does contain positively charged residues, it is missing two of the positive amino acids required for phosphoinositide binding. A canonical lysine on β -strand 1 of other PH domains is instead a leucine on ROCK1 and a canonical lysine on β -strand 2 of other PH

domains is valine on ROCK1. However, numerous basic residues on the surface form a charge distribution that might mediate its lipid binding activity [14].

ROCK1 is expected to have topological features similar to ROCK2's C1 domain which is cysteine rich, forming two zinc fingers and has 95% sequence similarity. The domain is composed of two beta sheets, one with 4 antiparallel β -strands and another antiparallel beta sheet composed of two β -strands. It is interesting to point out that ROCK1's and ROCK2's C1 domain contains a β -strand that is not typically seen in other C1 domains, with PKC being the exception [14]. ROCK1's C1 also differs in its zinc finger binding motif. Most C1 domains contain two CCHC zinc fingers, however, ROCK1 contains one CCHH and one CCHC motif. The residues involved in the CCHH zinc finger domain are Cys1266, Cys1269, His1292, and His1295. Residues coordinating the zinc ion in the CCHC domain are Cys1287, Cys1284, Cys1306, and His1252. Many C1 domains are known to bind DAG/phorbol esters but the C1 domain of ROCK1 lacks the sequence that corresponds to this activity. Rigidity and steric interference produced by hydrophobic residues Trp1273 and Met1275, as well as substitutions such as glycine in the essential sequence for lipid binding, are proposed to inhibit the capacity for ROCK's C1 domain to properly interact with DAG/phorbol esters [14]. There is a cluster of positively charged residues localized on the C1 domain which may act in tandem with the positive residues found in the PH domain allowing the two domains to exhibit a synergistic effect when binding to lipid membranes [14].

ROCK1 is known to form other important signaling complexes, such as with the Rho GTPase, RhoE, which it binds and inhibits. ROCK1 and RhoEs form this complex through hydrophobic contacts between the α EF Loop and α G helix of ROCK1 and the α 5 helix of RhoE [15] (Fig. 3). This allows ROCK to phosphorylate the Ser7 and Ser11 sites on RhoE [16]. Interestingly, the ROCK/RhoE complex is preferentially selective to the ROCK1 isoform, though Komander et al. [15] and Riento et al. [17] indicate that some ROCK2 binding and phosphorylation activity on RhoE is present. ROCKs have an insertion of residues Gly251 to Tyr254 that are unique relative to other kinases which form important interactions in the complex.

1.2. Auto-inhibition by PH domain

The catalytic domain of ROCK1 is inhibited by the Pleckstrin-Homology domain (PH domain) from residues 941 to 1388 [18,19] based on PH domain fragments that blocked stress fiber and focal adhesion formation in NIH 3T3 Cells. Furthermore, the PH domain is implicated in actomyosin assembly where a PH domain antibody was able to disrupt the assembly and cell contractility [20].

ROCK1 is activated in heart disease by low levels of activated Caspase 3 which cleaves ROCK1 at residue Asp1113, releasing the PH domain causing super-activated ROCK1, which may further enhance heart disease and fibrosis [4]. In addition, arachidonic acid is a ROCK1 activator [21].

Residues 998–1010 in the RBD bind RhoA-GTP [22,23] leading to activation. Rho binds to ROCK1 only in the activated

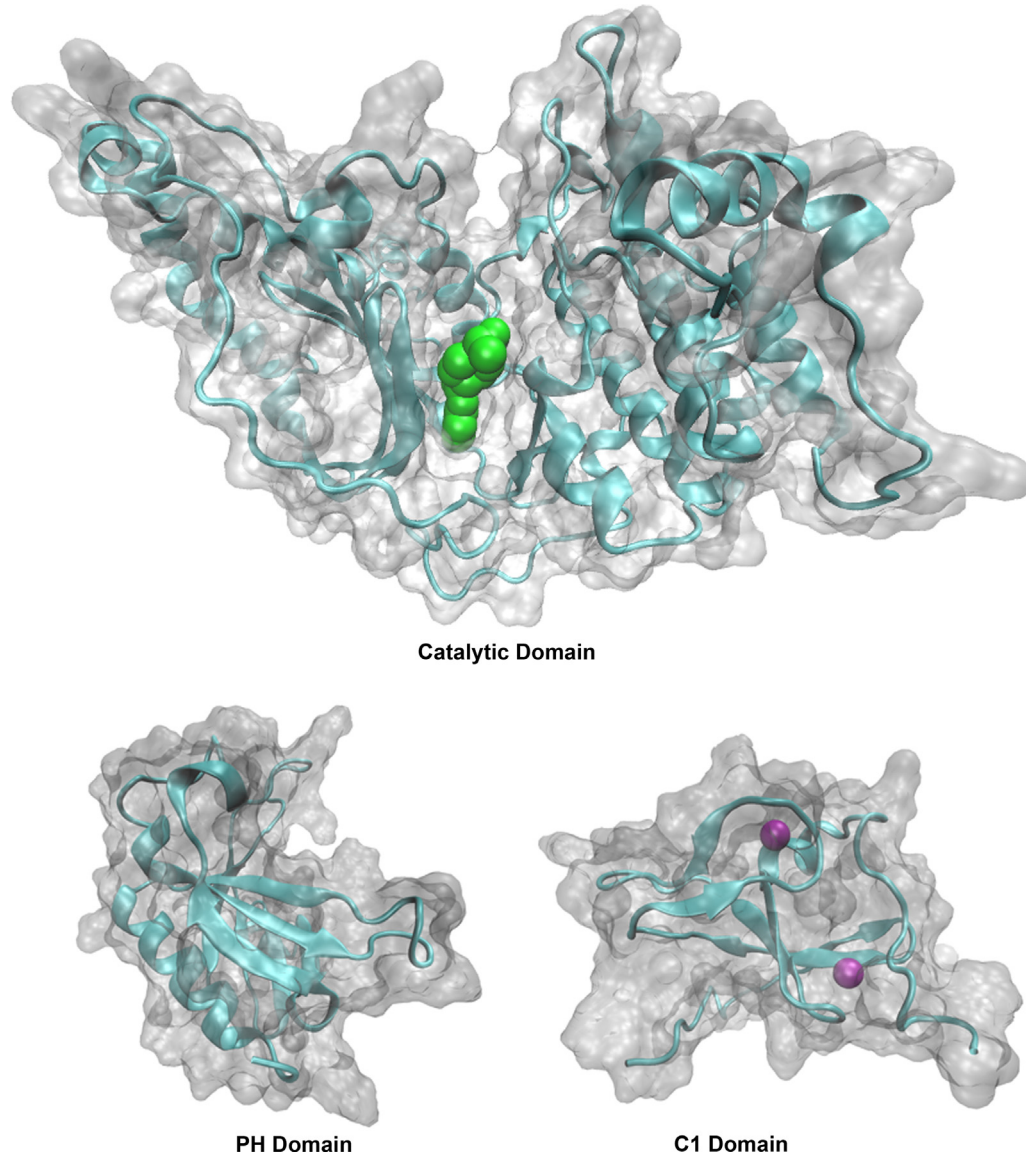


Fig. 2. (a) ROCK's catalytic domain crystal structure from Jacobs et al. [11] (PDB: 2ETR). Figure rendered in VMD [31] with Y27632 in green. (b) A surface rendering of the PH domain crystal structure from Wen et al. [14] (PDB: 2ROV) and b), the C1 Domain [14] (PDB: 2ROW). Rendered in VMD [31] with zinc ions purple.(For interpretation of the references to colour in this figure legend, the reader is referred to the web version of this article.)

GTP-bound complex [3]. The binding domain is found on a 13 residue coiled-coil helix composed of residues 998–1010 [23]. The hydrophobic residues in the ROCK1/RhoA interface that correspond to RhoA are Pro36, Val38, Phe39, Tyr66, Leu69, and Leu72. The hydrophobic residues that correspond to ROCK1 are Ala1002, Val1003, Leu1006, Ala1007, and Met1010 [23]. These residues form extensive contacts between the switch 1 and switch 2 regions of RhoA and each helix of the ROCK1 coiled-coil region, forming the main interactions that allow for protein binding. Residues Glu40, Asp65, and Arg68 of RhoA form hydrogen-bonds and electrostatic interactions with residues Lys1005, Lys999, and Asn1004 of ROCK1. Lys1005 forms a salt bridge, with a distance of 2.61 Å, within its own complex to Glu1008, allowing an electrostatic interaction between Lys1005 of ROCK1 and Glu40 of Rho A (3.07 Å distance) [23]. Arg68, which is 3.64 Å from Asn1004, forms a hydrogen-bond to the carbonyl group of Asn1004. Lys999 forms a 2.95 Å hydrogen-bond to Asp65 at the N-terminal end of the RBD [23]. These interactions allow for the appropriate orientation of two RhoA molecules with ROCK1's coiled-coil domain forming a stable complex to

activate ROCK1's catalytic kinase function. The coiled-coil domains from myotonic dystrophy kinase-related Cdc42-binding kinase and myotonic dystrophy protein kinase mediate clustering of dimers and higher order kinase groups [20] and may suggest an additional role for the coiled-coil domain in ROCK1.

The scope of published computational analysis of ROCK often focuses on small molecule drug design. Autodock was used to investigate the docking of 20 inhibitors in a recent study [24] which showed that these inhibitors bind in the ATP pocket. Docking was also used in a study of new indole and 7-azaindole inhibitors [25], however, in this work, we seek to evaluate protein-protein interactions between ROCK1's catalytic domain and its PH domain.

We hypothesize that ROCK1's autoinhibitory characteristics arise from self-association of its regulatory domains and its catalytic domain. Furthermore, understanding of the underlining mechanisms of ROCK recognition of its protein partners or substrates might lead to allosteric inhibitors or competitors that impinge on specific protein-protein interactions.

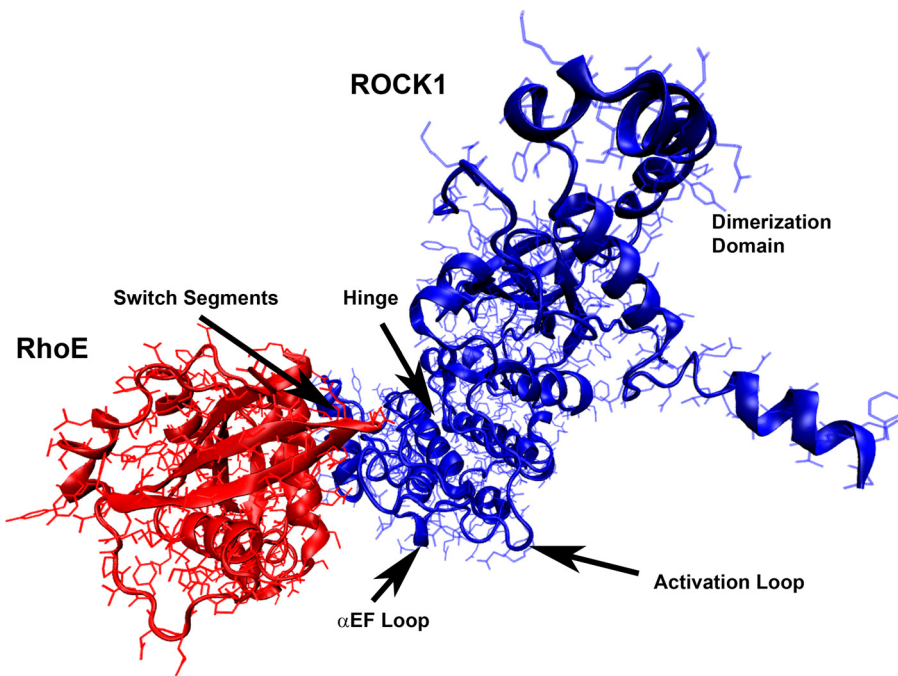


Fig. 3. Rho associated kinase (ROCK) catalytic domain in complex with RhoE from Komander et al. [15].

2. Materials and methods

2.1. Sequence and structure alignments of ROCK's PH domain

BLAST sequence alignments across a range of species and structure alignments of PH domains from other human proteins were analyzed to identify common features that might be important in complex formation. The species included gi#; 112382209, 1438567, 2982220, 1816620, and 24642569. These correspond to *Homo sapiens*, *Rattus rattus*, *Xenopus laevis*, *Caenorhabditis elegans*, and *Drosophila melanogaster*, respectively. Protein structures were aligned with known PH domains that included Pleckstrin (1PLS), AKT/RACa (2UZR), and PKBa (1UPQ) with an RMSD cutoff of 2. Additional sequence alignment of similar human kinases included ROCK2, MRCKg, Citron2, and Citron1. The hybrid alignment of sequence and structure data is supplemented with the matching feature information gleaned from the structure.

2.2. Surface plasmon resonance

To experimentally test whether the PH domain could form a complex with the catalytic domain, surface plasmon resonance (SPR) experiments were used to directly confirm the binding of the PH domain of ROCK1 with the catalytic domain of ROCK1. We developed a protocol to couple ROCK1 molecules to a CM5 sensor chip (Biacore 2000/GE Healthcare) using both direct amine coupling and by anti-His (C-term) antibody (Invitrogen 46-0693) where the antibody is coupled to the chip using amine chemistry following the manufacturer's requirements and the ROCK1 molecules are captured by its His-tag. This protocol orients the ROCK1 molecules so that the binding site is presented to the free flow in the micro channels enhancing the signal resolution. The PH domain was injected in 2× dilutions over the chip at 10 μL/min with a running buffer (PBS pH 7.4; 50 mM NaCl; 10 mM Na₂HPO₄; 2.7 mM KCl; 1.76 mM KH₂PO₄). Variations in NaCl concentration in PBS were prepared as low (50 mM), medium (150 mM) and high (300 mM). Negative controls were run using an injection of BSA, which is not expected to bind either the BSA blank in Fc1 or the ROCK1 in Fc2. All SPR

(Biacore sensorgrams) were analyzed from triplicate runs using a 1:1 Langmuir model in Scrubber (Version 2.0 Center for Biomolecular Interactions Analysis, University of Utah [26]).

The preparation of the CM5 Chip4 was primed three times with low salt PBS running buffer and wash for 1 min with 50 mM NaOH at 10 μL/min to precondition the surface. The Invitrogen anti-His AB was prepared to a target of 3000 RU as 8.3 μL diluted in 300 μL immobilization buffer (10 mM sodium acetate; pH = 6.1) based on pH scouting and protein isoelectric point. Immobilization of the anti-His AB in Fc3 as a reference and Fc4 to prepare for ROCK1-His-tag capture was completed (Supplemental Figure S1). A sample of ROCK1 catalytic domain (100 μg/mL stock) was prepared to 25 μg/mL by diluting 52 μL in 160 μL of immobilization buffer (10 mM sodium acetate; pH = 4.14) and immobilized on Fc2. Finally, a 100 mg/mL BSA stock was used to prepare 50 μg/mL sample by diluting 1 μL in 2 mL of immobilization buffer (10 mM sodium acetate; pH = 4.14). The chip was capped with a 150 μL injection of 1 M ethanolamine-HCl over Fc 1-2-3-4 manually.

2.3. Docking of the PH domain and the C1 subdomain

Possible complex geometries were explored using the Global Range Molecular Matching (GRAMM) [27,28] computational docking program. GRAMM is a coarse-grained docking method in which both the ligand and receptor are held rigid [29]. The docking against all six degrees of freedom can be explored in a rapid fashion using a Fast Fourier Transform (FFT) algorithm. The protein molecular surfaces are subject to a rough discretization in the form of a step potential. The intermolecular surfaces are scored on what is essentially a geometric fit based on a Lennard-Jones step potential. The end product is a series of scored ligand–receptor poses. The grid step was iterated on over the range of 2.0–6.8 Å. The number of seeds evaluated was set to 99 for each configuration. Clustering was completed using Matlab [30] scripts based on a K-means algorithm. Initial ROCK1 catalytic domain coordinates were obtained from the crystal structure of ROCK1 bound to Y-27632 (PDB: 2ETR) and ROCK1 bound to RhoE (PDB: 2V55). The 2ETR configuration was prepared by removing Y-27632 and the 2V55

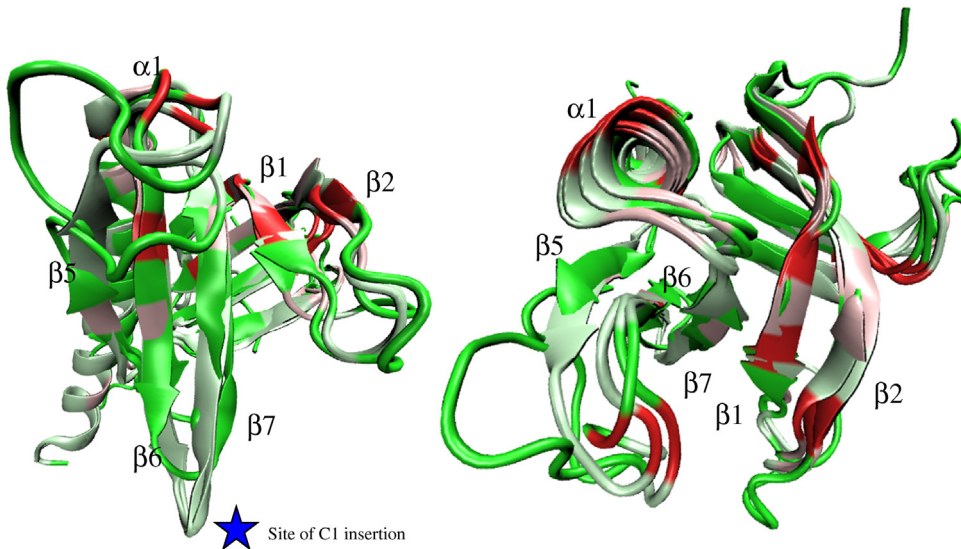


Fig. 4. A structure alignment of 1PLS Pleckstrin, 2UZR AKT/RACa, 1UPQ PKBa. The RMSD is less than the cutoff of 2.0 Å. Rendered in VMD in red/green/white color scale where identity is red and white is the largest residue root mean squared deviation (RMSD). (For interpretation of the references to colour in this figure legend, the reader is referred to the web version of this article.)

configuration was prepared by removing the AMP-PNP and Rho-E from the crystal structure of ROCK1. ROCK1's sequence from residues 1142 to 1342 form a split PH domain. The split PH domain of ROCK1 has been divided and sub-cloned into two subunits by Wen et al. [14] and solved by NMR spectroscopy. Their structure for the PH domain subunit (2ROV), residues 1142–1227 and residues 1312–1342 linked together with a single glycine was used as the model for a fully folded PH domain. Their structure for the C1 domain subunit (2ROW), residues 1228–1311, was used for docking against the ROCK catalytic domain. The leading seven residues of

the C1 domain subunit were removed as they are part of the flexible residues that connect the two subunits. It was found during initial docking that those residues contributed to large variances in docking poses because those residues are not part of the globular domain. A representative “best pose” from the most significant cluster in the first round of docking was then complexed with the catalytic domain and used in a second round of docking using the other remaining subunit leading to a full permutation of docking experiments of 2ROV and 2ROW as ligands to the catalytic domain (Table 1).

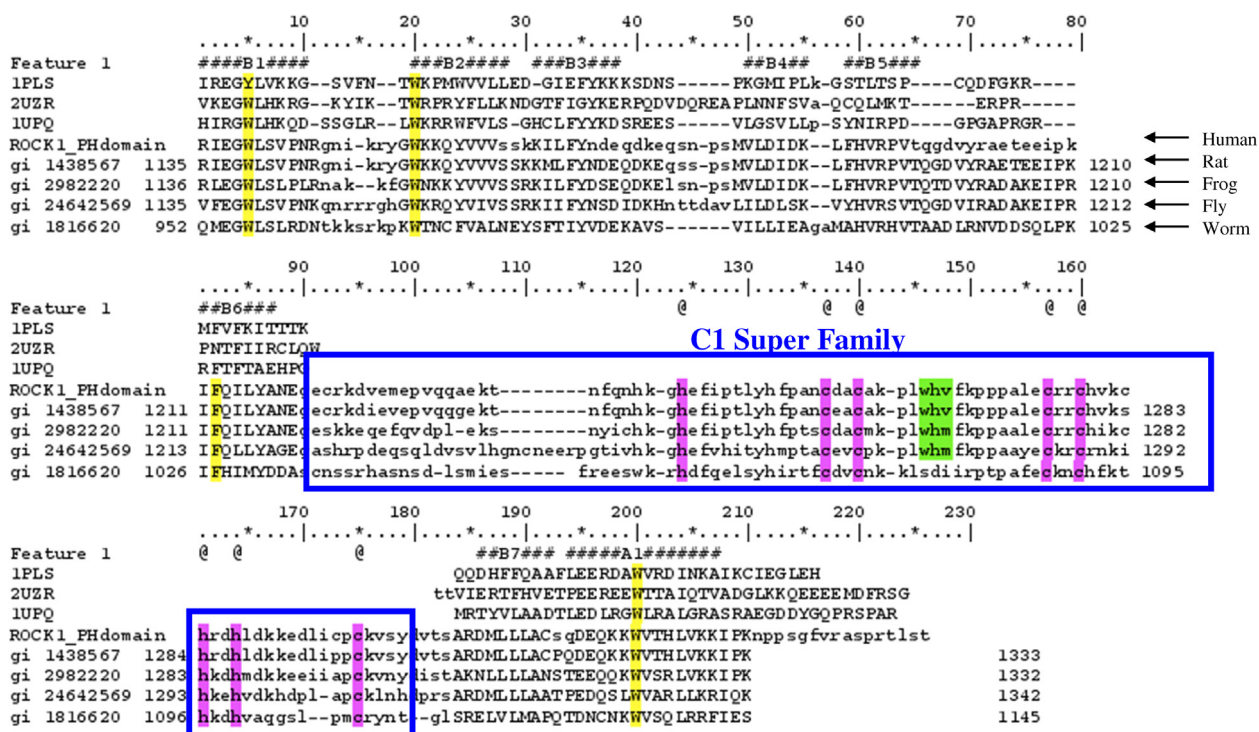


Fig. 5. A composite of sequence and structure alignments of ROCK1's split PH domain compared to other PH domains and other ROCK's in Human, Rat, Frog, Worm, and Fly. Yellow indicates key hydrophobic residues in the topology of the split PH domain, magenta are Cys and His residues that coordinate the zinc fingers, and green are the residues that occlude the ester binding site. (For interpretation of the references to colour in this figure legend, the reader is referred to the web version of this article.)

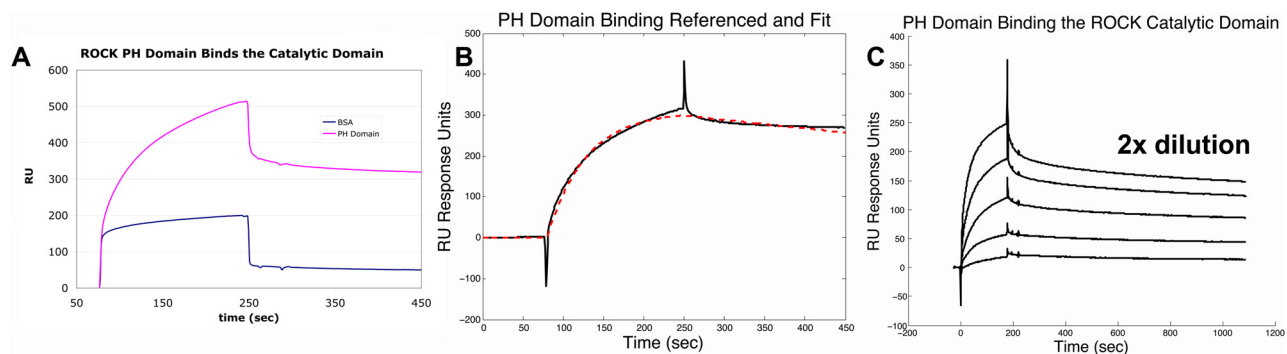


Fig. 6. (a) PH domain response curves. (b) Referenced Δ RU response for the PH domain with Fc 2 (ROCK1) – Fc1 (blank) and the Langmuir model in the red dashed line with a K_d of 1.22 μ M. (c) The Referenced Δ RU response from the SPR titration of PH domain on the ROCK1 catalytic domain with a 2 \times dilution and a concentration dependent response for PH domain binding to the ROCK1 catalytic domain. (For interpretation of the references to colour in this figure legend, the reader is referred to the web version of this article.)

Table 1
Initial coordinates of the ROCK1 structures.

| PDB ID | Description | Resolution (\AA) | Residue ID |
|--------|-----------------------------|-----------------------------|--------------------|
| 2ETR | ROCK1 bound to Y-27632 [11] | 2.6 | 6-402 |
| 2V55 | ROCK1 bound to RhoE [15] | 3.7 | 6-404 |
| 2ROV | PH domain [14] | NMR | 1142-12271312-1342 |
| 2ROW | C1 domain [14] | NMR | 1235-1311 |

3. Results

3.1. Sequence and structure alignments

The classic PH domain fold is preserved in ROCK1 with important conserved residues highlighted in red in Fig. 4. A combination of polar residues and key hydrophobic residues such as Phe82 and

Trp5, Trp20, and Trp200 preserve the packing of the α 1-helix and β 6-sheet.

A hybrid alignment of PH domains and ROCK specific domains are presented in Fig. 5, where the C1 domain insert is clear between β -strand 6 and β -strand 7. It is also interesting to see strong conservation of ROCK's split topology between organisms such as frogs, flies, and worms and that the known Cys and His residues that coordinate the zinc ions of the C1 domains are also conserved in all the species with ROCK. A comparison of the occluded phorbol ester binding site in ROCK between species suggests that all have residues WH(M/V)F, except *C. elegans* which has a SDII sequence.

3.2. Surface plasmon resonance

The binding of the PH domain of ROCK1 to the catalytic domain of ROCK1 was demonstrated by the Biacore response curves in

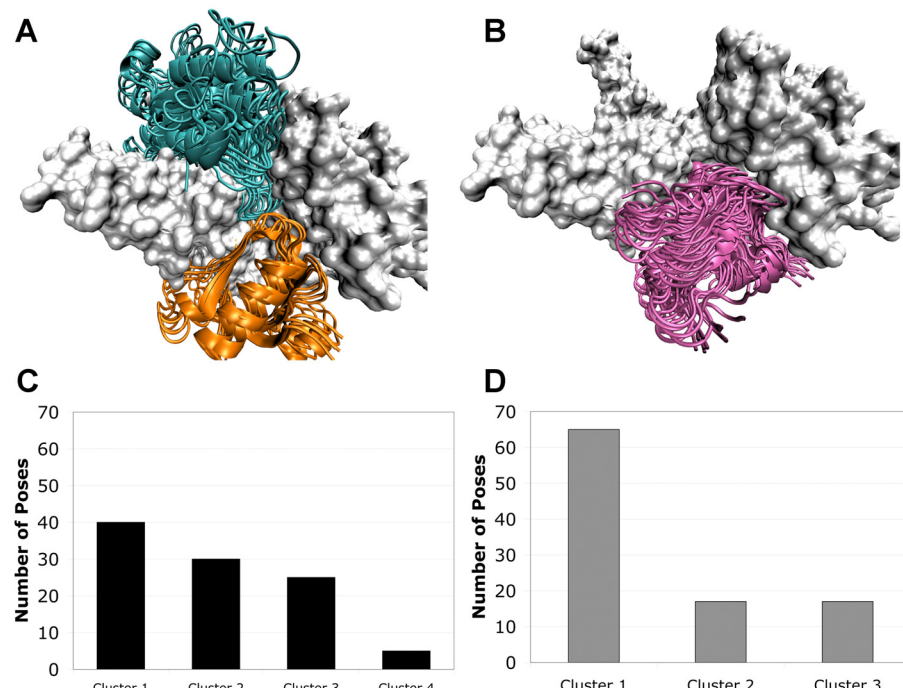


Fig. 7. (a) Two most-populated clusters are located where the PH domain subunit docks into the N-terminal lobe of the activation loop crevasse. A larger cluster is found near the distal end of the activation loop (blue-green) and the other is found on the face near the ATP binding site (orange). (b) The largest cluster of the C1 subunit docked on the face near the ATP binding site (mauve). (c) Histogram of PH domain clusters with 40% in the first cluster. (d) Histogram of C1 domain clusters with 65% of the population in the first cluster.

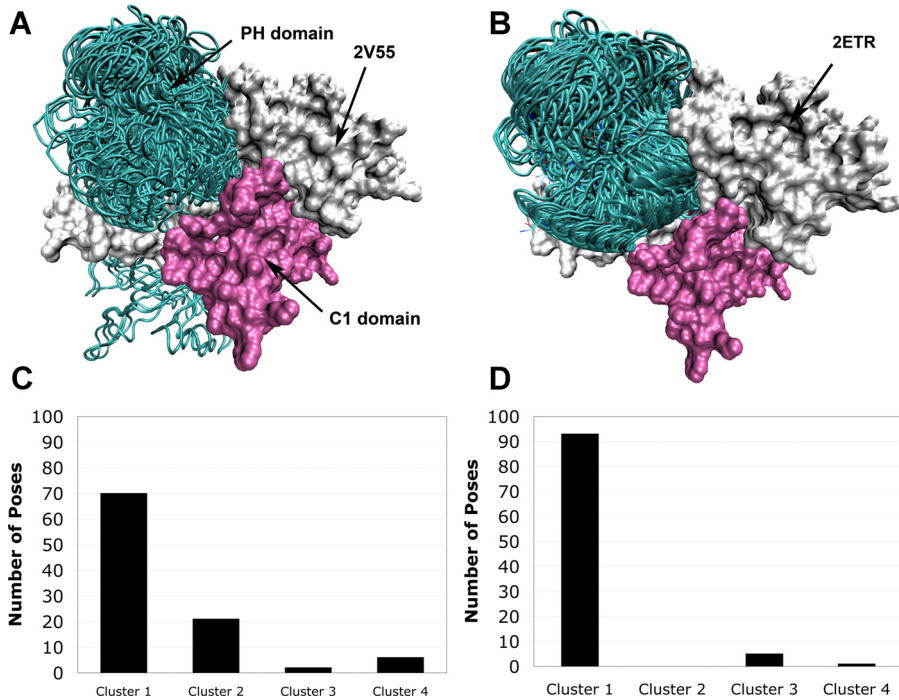


Fig. 8. ROCK PH domain docking: ROCK catalytic domain in white and the C1 domain in mauve based on the best representative C1 docked pose which was used as the target to dock the PH domain to test whether it would cluster in the similar region as when docked alone. (a) Where the target is 2V55. (b) The target is 2ETR. (c) The histogram of the clusters of 2V55. (d) The histogram of the clusters of 2ETR. The largest cluster of poses of the PH domain from both targets confirm that it can dock in complementary poses to the C1 domain to form a super complex.

Fig. 6. Some non-specific binding was observed in flow cell 1, which had BSA immobilized on it, however, it was much less than the binding characteristics in flow cell 2 (ROCK1 catalytic domain). The data were zeroed, aligned, and referenced. The binding is tight with a K_d of 1.22 μM (Fig. 6b) and a referenced ΔRU response of 260 remaining at 450 s while allowing the dissociation in the free running PBS buffer. A titration of PH domain was motivated by the initial positive binding results between the PH domain and the ROCK catalytic domain (Fig. 6c) and exhibits dose dependent binding. BSA injected as a control demonstrated that the non-specific interactions observed in all four flow cell (Fc)'s was limited and surface independent (Supplemental Figure S2).

3.3. Docking poses of the PH domain and the C1 subdomain

Computational docking identifies two complementary binding poses of ROCK1 split PH domain subunits. Interestingly, the two subunits of the ROCK1 split PH domain docked to the ROCK1 catalytic domain in separate regions with $<2\text{\AA}$ between them but allowing both to dock simultaneously. The binding poses elucidate a putative complex orientation where the PH domain subunit (Fig. 7a) and the C1 subunit (Fig. 7b) both dock against the ROCK1 catalytic domain and occlude the active site possibly deactivating ROCK1. We hypothesize that the largest cluster for the PH domain (blue-green Fig. 7a) and the largest cluster for the C1 domain

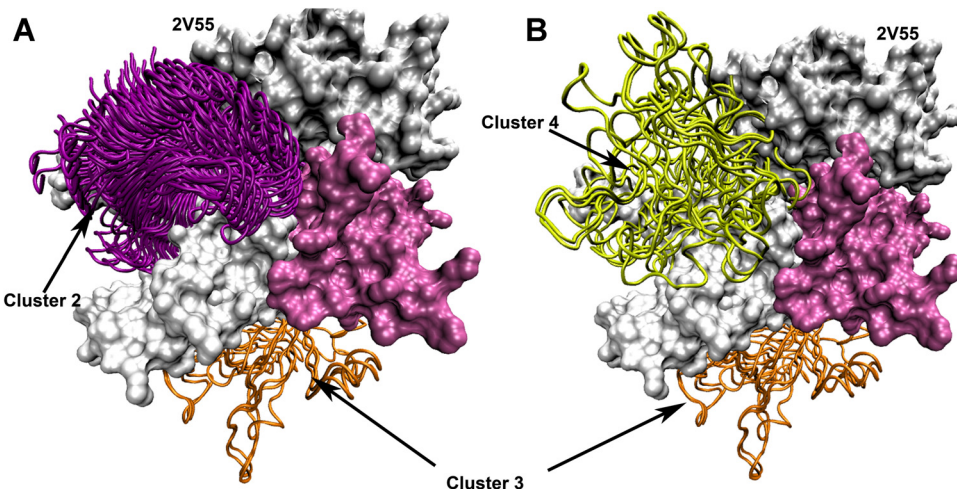


Fig. 9. ROCK PH domain docking of 2V55: cluster analysis in the super complex of the three domains shows cluster 2 can rotate into the space made available from the rotation of Ala234. Cluster 3 and 4 are dispersed small number of members on either the opposite face or in the cleft.

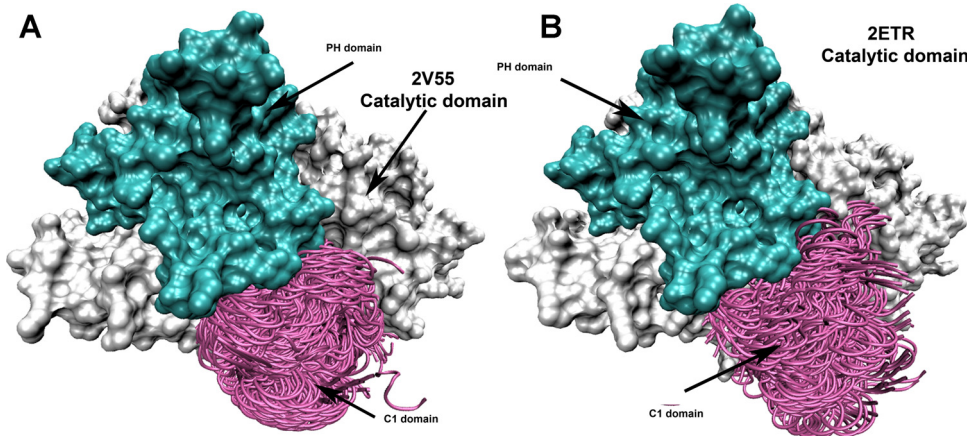


Fig. 10. ROCK C1 domain docking: ROCK catalytic domain in white and the PH domain in blue-green based on the best representative PH docked pose which was used as the target to dock the C1 domain to test whether it would cluster in the similar region as when docked alone. (a) The docking for 2V55. (b) The docking for 2ETR. The largest cluster of poses of the C1 domain confirm that it can also dock in complementary poses to the PH domain to form a super complex with both models. (For interpretation of the references to colour in this figure legend, the reader is referred to the web version of this article.)

(mauve Fig. 7b) can bind together with the ROCK1 catalytic domain forming a super complex of all three domains of ROCK1.

To further investigate whether ROCK1 can form a viable super complex with the catalytic domain we evaluated docking of both the PH domain and the C1 domain to a complex formed between the other one and the catalytic domain. Significant clustering of the PH domain in the hinge region and activation loop occurs when docked against the joint target of the catalytic/C1 domains for both scenarios where the catalytic domain was based on a model from 2V55 or 2ETR (Fig. 8a and b), similar to the earlier docking results when the PH domain was docked alone to the catalytic domain. Clustering of poses of the PH domain of the two dockings showed that 93% of them are in a complementary location in the cleft of the catalytic domain juxtaposed with the docking of the C1 domain when 2ETR was the target model (Fig. 8d). A similar percentage was present when 2V55 was the target, however, the more open space in the cleft allows more rotation variation in the docked poses. This can be seen as the number of poses that co-cluster with 2ETR's top ranked cluster was 70%, while 21% fall into a similar but shifted cluster 2 (Fig. 8c). Clusters 2, 3, and 4 from 2V55 are shown in Fig. 9 in which cluster 2 is allowed by the rotation of Ala234 (Supplemental Figure S3). Cluster 2 has an average RMSD variation from the top cluster of 18.6 ± 0.8 Angstroms. Cluster 3 is made up of only 2 members on an alternate face and cluster 4 is made up of 6 members with dispersed orientations in the cleft.

We then tested whether the docking of the C1 domain against a target complex of the catalytic/PH domain would reinforce the notion that the PH domain and the C1 domain can dock synergistically with the catalytic domain of ROCK1. In fact, a dense cluster (99%) docked in the same location as when the C1 was docked alone (Fig. 10a) for 2V55 and equivalently a cluster (88%) when 2ETR was the model.

3.4. Comparison of surface contact areas

The interface surfaces between the split PH domain/C1 domain and the ROCK1 catalytic domain was computed in VMD. The surface area in the C1 domain interface with the catalytic domain is 1289 \AA^2 , while the surface area in the PH domain interface with the catalytic domain is 1503 \AA^2 (Fig. 11). These data are in contrast to the surface area (483 \AA^2) in the interface between RhoE and the catalytic domain. Interestingly, the basic residues Lys43, Lys50, Lys71,

and Lys72 are on the solvent face of the protein complex. Additionally, Phe49, Trp46 and Pro35 and Pro44 are also on the solvent face. These basic and hydrophobic residues have been proposed to influence membrane localization.

Comparison of the docking of the C1 domain to the location of the RhoE interface in the 2V55 crystal structure indicates a steric clash of C1 domain's Lys16 and RhoE's Ile66. This is not unexpected as RhoE is a signaling partner of ROCK1 and is phosphorylated on Ser7 and Ser11 and is likely to interact with ROCK1 after ROCK1 is activated and the split PH domain is already disassociated.

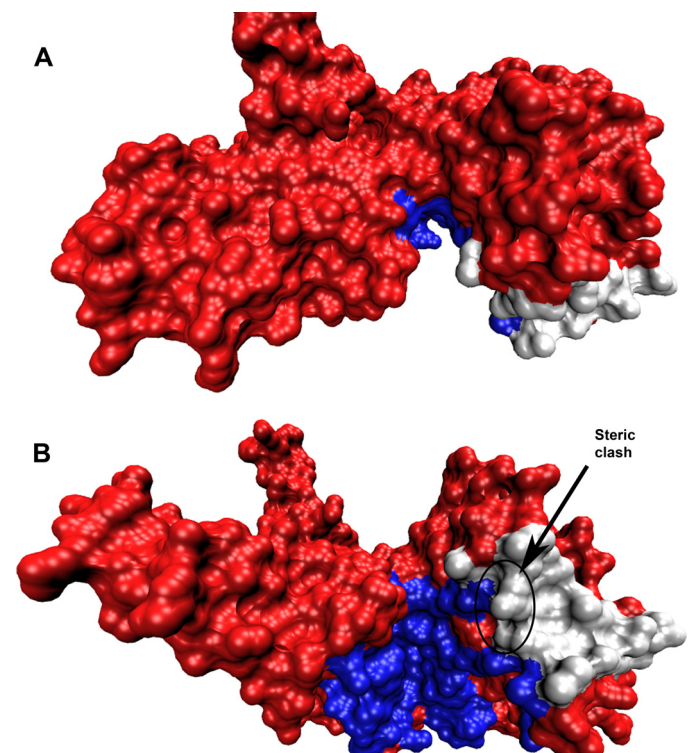


Fig. 11. (a). ROCK1 catalytic domain binding interfaces to the C1 domain (blue) area = 1289 \AA^2 , and RhoE GTPase (white) area = 483 \AA^2 . (b) Image rotated 180 degrees. (For interpretation of the references to colour in this figure legend, the reader is referred to the web version of this article.)

4. Conclusions

The split PH domain of Rho associated kinase-1 (ROCK1) has been shown to be involved in auto-inhibition of ROCK1 activity. The detailed mechanisms of how the inhibition is invoked remains under investigation. We sought to test whether a direct interaction of the C-terminal PH domain and the catalytic domain was possibly responsible for this auto-inhibition by occluding the active site. Our surface plasmon resonance data showed that there is binding between the catalytic domain and the split PH domain with a K_d of 1.22 μM . Having established binding experimentally, we then pursued computational docking studies to identify docked poses that might elucidate the complex. Wen et al. [14] established that each subunit in the split PH domain of ROCK1 folded independently, and so we first docked both the PH domain (2ROV) and the C1 domain (2ROW) individually against the catalytic domain and found that both could associate with favorable complimentary surfaces to form a complex. We then used the ROCK1 catalytic/C1 complex as a target and computationally tested whether the PH domain would still cluster to form a super complex between all three domains. Furthermore we also tested the alternative docking target of a complex formed by the ROCK1 catalytic/PH domain and evaluated the C1 domain which also formed a similar super complex. Both the PH domain and the C1 domain did cluster in the same proximity when docked alone or in complex with the other. This result was observed for both scenarios when either 2V55 or 2ETR was used as the model for the catalytic domain of ROCK1. This strengthens the idea that the split PH domain could form a super complex with interactions along the hinge region of the kinase catalytic domain, occluding the active site, and making extensive contacts with the activation loop. Our results provide a strong rationale for how ROCK1's auto-inhibition is mediated and possible clues to how it is regulated.

Acknowledgements

RJS would like to thank the Norman Hackerman Advanced Research Program in the State of Texas for partial support of this work. Gratitude is expressed to the University of Houston Texas Learning and Computation Center and the Research Computing Center for computational resources.

Appendix A. Supplementary data

Supplementary data associated with this article can be found, in the online version, at <http://dx.doi.org/10.1016/j.jmgm.2013.09.009>.

References

- [1] J. Narula, E. Arbustini, Y. Chandrashekhar, M. Schwaiger, Apoptosis and the systolic dysfunction in congestive heart failure: story of apoptosis interruptus and zombie myocytes, *Cardiology Clinics* 19 (1) (2001) 113–126.
- [2] S.B. Haudek, D. Gupta, O. Dewald, R.J. Schwartz, L. Wei, J. Trial, M.L. Entman, Rho kinase-1 mediates cardiac fibrosis by regulating fibroblast precursor cell differentiation, *Cardiovascular Research* 83 (3) (2009) 511–518.
- [3] T.M.M. Ishizaki, K. Fujisawa, K. Okawa, A. Iwamatsu, A. Fujita, N. Watanabe, Y. Saito, A. Kakizuka, N. Morii, S. Narumiya, The small GTP-binding protein Rho binds to and activates a 160 kDa Ser/Thr protein kinase homologous to myotonic dystrophy kinase, *EMBO Journal* 15 (8) (1996) 1885–1893.
- [4] J. Chang, M. Xie, V.R. Shah, M.D. Schneider, M.L. Entman, L. Wei, R.J. Schwartz, Activation of Rho associated coiled-coiled protein kinase 1 (ROCK-1) by caspase-3 cleavage, *Proceedings of the National Academy of Sciences of the United States of America* 103 (39) (2006) 14495–14500.
- [5] Y.-M. Zhang, J. Bo, G.E. Taffet, J. Chang, J. Shi, A.K. Reddy, L.H. Michael, M.D. Schneider, M.L. Entman, R.J. Schwartz, L. Wei, Targeted deletion of ROCK1 protects the heart against pressure overload by inhibiting reactive fibrosis, *FASEB Journal* 20 (7) (2006) 916–925.
- [6] L. Wei, G.E. Taffet, D.S. Khoury, J. Bo, Y. Li, A. Yatani, M.C. Delaughter, R. Klevitsky, T.E. Hewett, J. Robbins, L.H. Michael, M.D. Schneider, M.L. Entman, R.J. Schwartz, Disruption of Rho signaling results in progressive atrioventricular conduction defects while ventricular function remains preserved, *FASEB Journal* 18 (7) (2004) 857–859.
- [7] L. Wei, K. Imanaka-Yoshida, L. Wang, S. Zhan, M.D. Schneider, F.J. DeMayo, R.J. Schwartz, Inhibition of Rho family GTPases by Rho GDP dissociation inhibitor disrupts cardiac morphogenesis and inhibits cardiomyocyte proliferation, *Development* 129 (7) (2002) 1705–1714.
- [8] L. Wei, W. Roberts, L. Wang, M. Yamada, S. Zhang, Z. Zhao, S.A. Rivkees, R.J. Schwartz, K. Imanaka-Yoshida, Rho kinases play an obligatory role in vertebrate embryonic organogenesis, *Development* 128 (15) (2001) 2953–2962.
- [9] O. Nakagawa, K. Fujisawa, T. Ishizaki, Y. Saito, K. Nakao, S. Narumiya, ROCK-I and ROCK-II, two isoforms of Rho-associated coiled-coil forming protein serine/threonine kinase in mice, *FEBS Letters* 392 (2) (1996) 189–193.
- [10] D. Thumkeo, J. Keel, T. Ishizaki, M. Hirose, K. Nonomura, H. Oshima, M. Oshima, M.M. Takeo, S. Narumiya, Targeted disruption of the mouse rho-associated kinase 2 gene results in intrauterine growth retardation and fetal death, *Molecular and Cellular Biology* 23 (14) (2003) 5043–5055.
- [11] M. Jacobs, K. Hayakawa, L. Swenson, S. Bellon, M. Fleming, P. Taslimi, J. Doran, The structure of dimeric ROCK I reveals the mechanism for ligand selectivity, *Journal of Biological Chemistry* 281 (1) (2006) 260–268.
- [12] H. Yamaguchi, M. Kasa, M. Amano, K. Kaibuchi, T. Hakoshima, Molecular mechanism for the regulation of Rho-kinase by dimerization and its inhibition by Fasudil, *Structure* 14 (3) (2006) 589–600.
- [13] B.K. Mueller, H. Mack, N. Neusch, Rho kinase, a promising drug target for neurological disorders, *Nature Reviews Drug Discovery* 4 (5) (2005) 387–398.
- [14] W. Wen, W. Liu, J. Yan, M. Zhang, Structure basis and unconventional lipid membrane binding properties of the PH-C1 tandem of Rho kinases, *Journal of Biological Chemistry* 283 (38) (2008) 26263–26273.
- [15] D. Komander, R. Garg, P.T.C. Wan, A.J. Ridley, D. Barford, Mechanism of multi-site phosphorylation from a ROCK-I:RhoE complex structure, *EMBO Journal* 27 (23) (2008) 3175–3185.
- [16] K. Riento, N. Totty, P. Villalonga, R. Garg, R. Guasch, A.J. Ridley, RhoE function is regulated by ROCK-I-mediated phosphorylation, *EMBO Journal* 24 (6) (2005) 1170–1180.
- [17] K. Riento, A.J. Ridley, C.J.D. William, E. Balch, H. Alan, Inhibition of ROCK by RhoE, in: *Methods in Enzymology*, Academic Press, 2006, pp. 533–541.
- [18] M. Amano, K. Chihara, K. Kimura, Y. Fukata, N. Nakamura, Y. Matsuura, K. Kaibuchi, Formation of Actin stress fibers and focal adhesions enhanced by Rho-Kinase, *Science* 275 (5304) (1997) 1308–1311.
- [19] M. Amano, K. Chihara, N. Nakamura, T. Kaneko, Y. Matsuura, K. Kaibuchi, The COOH terminus of Rho-kinase negatively regulates Rho-kinase activity, *Journal of Biological Chemistry* 274 (45) (1999) 32418–32424.
- [20] X.-q. Chen, I. Tan, C.H. Ng, C. Hall, L. Lim, T. Leung, Characterization of RhoA-binding kinase ROK α : implication of the Pleckstrin homology domain in ROK α function using region-specific antibodies, *Journal of Biological Chemistry* 277 (15) (2002) 12680–12688.
- [21] J. Feng, M. Ito, Y. Kureishi, K. Ichikawa, M. Amano, N. Isaka, K. Okawa, A. Iwamatsu, K. Kaibuchi, D.J. Hartshorne, T. Nakano, Rho-associated kinase of chicken gizzard smooth muscle, *Journal of Biological Chemistry* 274 (274) (1999) 3744–3752.
- [22] T. Shimizu, K. Ihara, R. Maesaki, M. Amano, K. Kaibuchi, T. Hakoshima, Parallel coiled-coil association of the RhoA-binding domain in Rho-kinase, *Journal of Biological Chemistry* 278 (46) (2003) 46046–46051.
- [23] R. Dvorsky, L. Blumenstein, I.R. Vetter, M.R. Ahmadian, Structural insights into the interaction of ROCKI with the switch regions of RhoA, *Journal of Biological Chemistry* 279 (8) (2004) 7098–7104.
- [24] D.-H. Wang, W.-L. Qu, L.-Q. Shi, J. Wei, Molecular docking and pharmacophore model studies of Rho kinase inhibitors, *Molecular Simulation* 37 (06) (2011) 488–494.
- [25] S. Chowdhury, E.H. Sessions, J.R. Pocas, W. Grant, T. Schr.Øter, L. Lin, C. Ruiz, M.D. Cameron, S. Sch.Øter, P. LoGrasso, T.D. Bannister, Y. Feng, Discovery and optimization of indoles and 7-azaindoles as Rho kinase (ROCK) inhibitors (part-I), *Bioorganic & Medicinal Chemistry Letters* 0 (2011).
- [26] U.O. Utah, Scrubber, Center for Biomolecular Interactions Analysis, 2003.
- [27] I.A. Vakser, Low-resolution docking: prediction of complexes for underdetermined structures, *Biopolymers* 39 (3) (1996) 455–464.
- [28] I.A. Vakser, Evaluation of GRAMM low-resolution docking methodology on the hemagglutinin-antibody complex, *Proteins: Structure, Function, and Bioinformatics* 1 (1997) 226–230.
- [29] I.A. Vakser, O.G. Matar, C.F. Lam, A systematic study of low-resolution recognition in protein-protein complexes, *Proceedings of the National Academy of Science* 96 (15) (1999) 8477–8482.
- [30] Mathworks, T. Matlab.
- [31] W. Humphrey, A. Dalke, K. Schulten, VMD: visual molecular dynamics, *Journal of Molecular Graphics* 14 (1) (1996), 33–8, 27–8.